A protective role for the A_1 adenosine receptor in adenosine-dependent pulmonary injury

Chun-Xiao Sun,[1] Hays W. Young,[1] Jose G. Molina,[1] Jonathan B. Volmer,[1] Jurgen Schnermann,[2] and Michael R. Blackburn[1]

[1]Department of Biochemistry and Molecular Biology, University of Texas Health Science Center at Houston Medical School, Houston, Texas, USA.
[2]National Institute of Diabetes and Digestive and Kidney Diseases, NIH, Bethesda, Maryland, USA.

Adenosine is a signaling nucleoside that has been implicated in the regulation of asthma and chronic obstructive pulmonary disease. Adenosine signaling can serve both pro- and anti-inflammatory functions in tissues and cells. In this study we examined the contribution of A_1 adenosine receptor (A_1AR) signaling to the pulmonary inflammation and injury seen in adenosine deaminase–deficient (ADA-deficient) mice, which exhibit elevated adenosine levels. Experiments revealed that transcript levels for the A_1AR were elevated in the lungs of ADA-deficient mice, in which expression was localized predominantly to alveolar macrophages. Genetic removal of the A_1AR from ADA-deficient mice resulted in enhanced pulmonary inflammation along with increased mucus metaplasia and alveolar destruction. These changes were associated with the exaggerated expression of the Th2 cytokines IL-4 and IL-13 in the lungs, together with increased expression of chemokines and matrix metalloproteinases. These findings demonstrate that the A_1AR plays an anti-inflammatory and/or protective role in the pulmonary phenotype seen in ADA-deficient mice, which suggests that A_1AR signaling may serve to regulate the severity of pulmonary inflammation and remodeling seen in chronic lung diseases by controlling the levels of important mediators of pulmonary inflammation and damage.

Introduction

Asthma and chronic obstructive pulmonary disease (COPD) are pulmonary disorders that afflict millions of people and result in a substantial economic burden to the US health care system. Although these disorders have unique and distinguishing features, they both exhibit persistent airway inflammation and airway remodeling that can lead to the progressive loss of lung function (1, 2). Whereas cellular and signaling processes that lead to initial inflammatory cascades in asthma and COPD have been well studied, less is known about the pathways associated with asthma exacerbations or airway remodeling. Examining signaling pathways that are involved in the regulation of acute and chronic inflammatory and remodeling events in the lung will be important for the development of new treatment options for these pulmonary disorders.

Adenosine is a regulatory nucleoside that is generated in response to cellular stress and damage and is therefore increased during episodes of tissue hypoxia and inflammation. Levels of adenosine are increased in the lungs of asthmatics (3), in which elevations correlate with the degree of inflammatory insult (4). Existing evidence suggests that adenosine may play a provocative role in asthma and COPD (5, 6). Adenosine or its precursor, AMP, can elicit bronchoconstriction in asthmatic (7) and COPD patients (8) while having little effect on normal individuals. In asthmatics, this response appears to be mediated by adenosine-induced mast cell degranulation in the airways (9, 10). These data point to a proinflammatory role for adenosine during the acute phases of asthma. Recent studies in genetically modified mice suggest that adenosine also contributes to chronic attributes of pulmonary injury, including the promotion of persistent airway inflammation, alveolar destruction, and pulmonary fibrosis (11, 12). Thus, adenosine represents a signaling molecule that may couple the degree of damage in the lung to pathways that promote the progression of lung injury.

A proinflammatory and/or disease-progressing role for adenosine in asthma and COPD is in opposition to the well-established actions of adenosine as an anti-inflammatory and tissue protective signal in acute inflammatory responses such as those seen following ischemia reperfusion injury or endotoxin exposure (reviewed in refs. 13, 14). Distinct pro- and anti-inflammatory roles of adenosine are likely mediated by the expression profile of specific adenosine receptors (ARs) on specific cells. Four ARs have been identified: A_1AR, A_{2A}AR, A_{2B}AR, and A_3AR (15). These receptors consist of 7 membrane-spanning proteins that couple to heterotrimeric G proteins to access numerous intracellular signaling pathways. Inflammatory cytokines can alter the expression of ARs in various cell types (16, 17), which suggests that adenosine-signaling parameters are dynamic in inflammatory environments. Thus, distinguishing pro- and anti-inflammatory functions of adenosine will involve understanding the regulation and actions of specific ARs on specific cell types in different inflammatory environments. Efforts to define AR-specific activities in various environments will help to guide the use of receptor-specific agonists and antagonists in the treatment of various inflammatory disorders.

The A_1AR has a high affinity for adenosine and has been implicated in both pro- and anti-inflammatory aspects of disease processes. For example, some studies have shown that A_1AR signaling can promote neutrophil (18) and monocyte activation (19, 20) while others have suggested that A_1AR signaling is involved in anti-inflammatory and protective pathways in neuroinflammation and injury (21), and in cardiac (22) and renal (23, 24) injury. In the lung, A_1AR activation has been implicated in the regulation of

Nonstandard abbreviations used: ADA, adenosine deaminase; AR, adenosine receptor; BAL, bronchial alveolar lavage; BALF, BAL fluid; COPD, chronic obstructive pulmonary disease; mCLCA3, mouse calcium-activated chloride channel 3; TARC, thymus- and activation-regulated chemokine.

Conflict of interest: The authors have declared that no conflict of interest exists.

Citation for this article: *J. Clin. Invest.* **115**:35–43 (2005). doi:10.1172/JCI200522656.

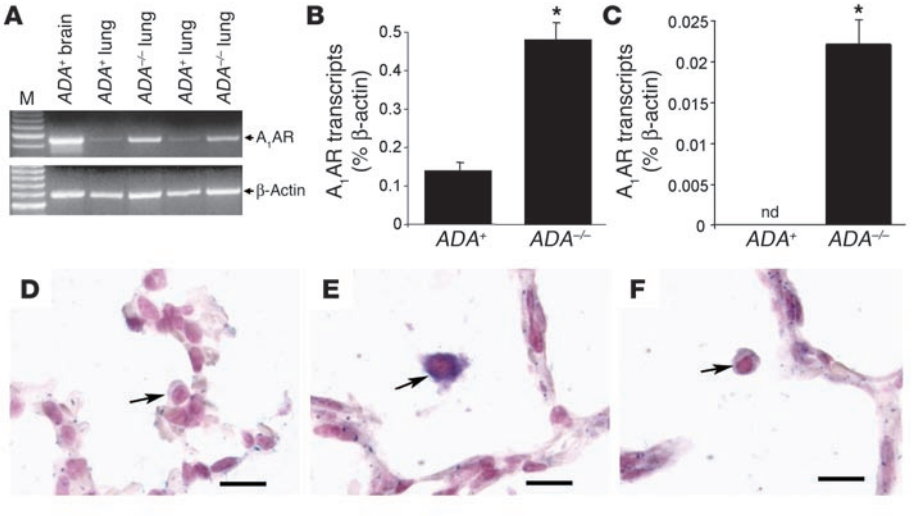

Figure 1

A1AR expression in the lungs of *ADA*$^{-/-}$ mice. (**A**) Transcript levels for the A_1AR were measured in whole-lung RNA extracts from postnatal day 18 ADA-containing (*ADA*$^{+}$) and ADA-deficient (*ADA*$^{-/-}$) mice, using semiquantitative RT-PCR. Findings from 2 different pairs of littermates are shown. RNA extracted from the brain of an *ADA*$^{+}$ mouse was used as a positive control, and β-actin was used as an RNA-positive control for each sample. M, DNA size ladder. Quantitative RT-PCR was used to determine the levels of *A1AR* transcripts in day 18 whole-lung extracts (**B**) or BAL cell pellets (**C**) from *ADA*$^{+}$ and *ADA*$^{-/-}$ mice. Data are presented as mean percentage of β-actin transcripts ± SEM; $n = 4$ for each. *$P \leq 0.05$ compared to *ADA*$^{+}$. nd, not detectable. Images show (**D**) lung section from a postnatal day 18 *ADA*$^{+}$ mouse hybridized with antisense A_1AR riboprobe, (**E**) lung section from a postnatal day 18 *ADA*$^{-/-}$ mouse hybridized with antisense A_1AR riboprobe, and (**F**) lung section from a postnatal day 18 *ADA*$^{-/-}$ mouse hybridized with sense A_1AR riboprobe. Purple represents specific hybridization; pink shows counterstained nuclei. Arrows denote alveolar macrophages. Scale bar: 10 μm.

bronchoconstriction in allergic rabbit models (25–27), suggesting a provocative role for A_1AR signaling in acute phases of asthma. Similarly, A_1AR receptor antagonism has been shown to be beneficial in attenuating ischemia reperfusion (28) and endotoxin-induced (29) lung injury, suggesting a proinflammatory role for A_1AR signaling in acute lung injury. However, the role of the A_1AR in inflammation and injury processes seen in chronic phases of pulmonary disease has not been examined.

We have developed a model of adenosine-mediated pulmonary injury that has allowed us to examine the consequences of adenosine elevations to pulmonary inflammation and injury. Adenosine deaminase (ADA) is the purine catabolic enzyme responsible for the deamination of adenosine to inosine, and mice that lack this enzyme develop aspects of chronic pulmonary injury in association with elevations in lung adenosine levels (11). Pulmonary features seen include mast cell degranulation, progressive airway inflammation characterized by elevations in airway macrophages and eosinophils, mucus metaplasia, airway enlargement, fibrosis, and airway hyperreactivity (11, 30, 31). This model has proven useful in the examination of specific signaling pathways involved in adenosine-mediated pulmonary injury (32, 33). In the current study, we examined the function of the A_1AR in adenosine-mediated pulmonary inflammation and injury by the genetic removal of the functional *A1AR* gene from ADA-deficient mice. Results indicate that the A_1AR serves an anti-inflammatory role in the development of pulmonary inflammation and alveolar destruction in ADA-deficient mice, which suggests a protective role for this receptor in the regulation of pulmonary disorders in which adenosine levels are elevated.

Results

A1AR transcripts are elevated in the lungs of ADA$^{-/-}$ *mice*. Semiquantitative RT-PCR was performed to determine the levels of *A1AR* transcripts in the lungs of ADA-deficient (*ADA*$^{-/-}$) mice. *A1AR* transcripts were detectable in the lungs of ADA-containing (*ADA*$^{+}$) and *ADA*$^{-/-}$ mice, with an apparent increase in the lungs of *ADA*$^{-/-}$ mice (Figure 1A). These findings were confirmed using quantitative RT-PCR, which demonstrated a mean 3-fold increase of *A1AR* transcripts in whole-lung RNA extracts (Figure 1B) and a 50-fold increase in *A1AR* transcripts in RNA isolated from bronchial alveolar lavage (BAL) cell pellets from *ADA*$^{-/-}$ mice (Figure 1C). Localization studies demonstrated that *A1AR* transcripts were not detectable in the lungs of *ADA*$^{+}$ mice; however, *A1AR* transcripts were detectable in various cell types in the lungs of *ADA*$^{-/-}$ mice. Hybridization signal was detected in most alveolar macrophages (Figure 1E) in the lungs of *ADA*$^{-/-}$ mice with occasional signal found in endothelial cells, airway epithelial cells, and alveolar epithelial cells (data not shown). These findings demonstrate that *A1AR* transcripts are elevated in multiple cell types in the lungs of *ADA*$^{-/-}$ mice.

Lung inflammation is exacerbated in ADA/A1AR double-knockout mice. *ADA*$^{-/-}$ mice develop lung inflammation at postnatal day 10 when increases in alveolar macrophages are the most prominent feature (11). This inflammation is progressive, with eosinophilia and alveolar destruction being found at postnatal day 18; *ADA*$^{-/-}$ mice die between days 18 and 21 in association with severe respiratory distress. Mice lacking both *ADA* and the *A1AR* (*ADA/A1AR* double-knockout mice) were generated to examine the contribution of A_1AR signaling to the pulmonary phenotype seen in *ADA*$^{-/-}$ mice. Initial observations demonstrated that removal of the *A1AR* was associated with a precocious onset of respiratory distress and death in *ADA*$^{-/-}$ mice. *ADA/A1AR* double-knockout mice developed outward symptoms of respiratory distress by postnatal day 12 and died on postnatal day 15 or 16 (data not shown). Subsequent analysis of *ADA* and *A1AR* single- and double-knockout mice was therefore conducted on postnatal day 14. Histological examination of the lungs demonstrated that mice containing *ADA* but lacking the *A1AR* had normal lung architecture and no evidence of lung inflammation (Figure 2B). *ADA*$^{-/-}$ mice containing the *A1AR* had diffuse monocytic inflammation and enlargement of the alveolar airways (Figure 2C) while *ADA/A1AR* double-knockout mice exhibited accelerated pulmonary inflammation (Figure 2D). Consistent with this observation, there was a significant increase in the number of inflammatory cells recovered from the BAL fluid (BALF) of *ADA/A1AR* double-knockout mice as compared to that seen in the lungs of *ADA*$^{-/-}$ mice containing the *A1AR* (Figure 3A). Significant increases in numbers of eosinophils, neutrophils, and lymphocytes were seen (Figure 3B) as well as increases in numbers of alveolar

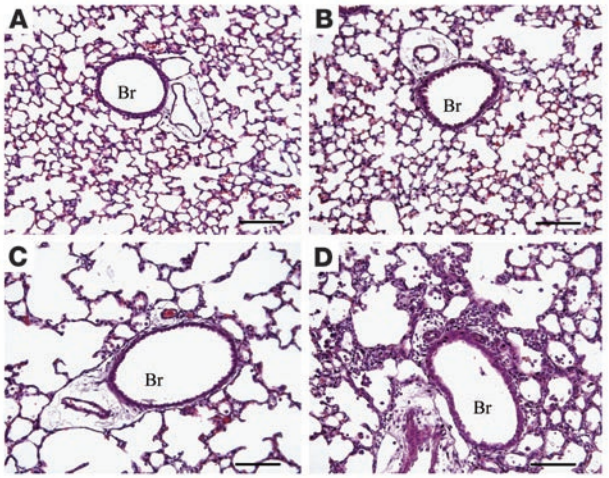

Figure 2
Histological findings in the lungs of *ADA/A$_1$AR* double-knockout mice. Lungs were collected on postnatal day 14 and processed for H&E staining. Images show (**A**) lung from an *ADA$^+$A$_1$AR$^{+/+}$* mouse, (**B**) lung from an *ADA$^+$A$_1$AR$^{-/-}$* mouse, (**C**) lung from an *ADA$^{-/-}$A$_1$AR$^{+/+}$* mouse, and (**D**) lung from an *ADA$^{-/-}$A$_1$AR$^{-/-}$* mouse. Images are representative of 10 animals from each group. Scale bar: 100 μm. Br, bronchiole.

macrophages, many of which were enlarged foam cells (Figure 3C). These findings demonstrate that removal of the *A$_1$AR* in *ADA$^{-/-}$* mice is associated with enhanced pulmonary inflammation.

Increased mucus metaplasia in the lungs of ADA/A$_1$AR double-knockout mice. Previous studies have demonstrated the existence of mucus metaplasia in the bronchial airways of *ADA$^{-/-}$* mice (11). To determine the contribution of A$_1$AR signaling to mucus metaplasia in this model, we examined the production of mucus in the airways of *ADA/A$_1$AR* double-knockout mice. *ADA$^{-/-}$* mice containing the *A$_1$AR* exhibited mucus metaplasia in their bronchial airways at postnatal day 14 as determined by PAS staining (Figure 4, C and E). Removal of the *A$_1$AR* resulted in a significant increase in mucus metaplasia in the airways of *ADA$^{-/-}$* mice (Figure 4, D and E). We next examined transcript levels of key mucus-associated genes in whole-lung RNA extracts. Transcript levels for the mucins Muc5ac and Muc5b were elevated in the lungs of *ADA$^{-/-}$* mice with and without the *A$_1$AR*, but only Muc5b was significantly increased in the absence of the *A$_1$AR* (Figure 4F). Similarly, transcript levels for the mouse calcium-activated chloride channel 3 (mCLCA3) were substantially increased in the lungs of *ADA$^{-/-}$* mice following the removal of the *A$_1$AR* (Figure 4F). These findings demonstrate that mucus metaplasia is enhanced in the lungs of *ADA$^{-/-}$* mice lacking the A$_1$AR.

Increased cytokine and chemokine production in the lungs of ADA/A$_1$AR double-knockout mice. To explore the involvement of proinflammatory mediators in the enhanced pulmonary inflammation seen in *ADA/A$_1$AR* double-knockout mice, cytokine and chemokine transcript levels were monitored in whole-lung RNA extracts. Transcript levels for IL-4 were not elevated in the lungs of *ADA$^{-/-}$* mice containing the *A$_1$AR*; however, they were significantly elevated in the lungs of *ADA/A$_1$AR* double-knockout mice (Figure 5). *IL-13* transcripts were elevated in the lungs of *ADA$^{-/-}$* mice, and levels were markedly elevated in the absence of the *A$_1$AR* (Figure 5). *IL-6* transcripts were elevated in the lungs of *ADA$^{-/-}$* mice but did not change with the removal of the *A$_1$AR* (Figure 5). Among the chemokines examined, levels of eotaxin 2 and thymus- and activation-regulated chemokine (TARC) were found to be markedly increased in the lungs of *ADA/A$_1$AR* double-knockout mice (Figure 6). Transcript levels of other cytokines and chemokines (IL-5, IL-9, IL-17, TNF-α, TGF-β1, IFN-γ, Rantes, and CCR3) were examined but were found not to have changed (data not shown). These data demonstrate that removal of the *A$_1$AR* results in exaggerated expression of IL-4, IL-13, eotaxin 2, and TARC in the lungs of *ADA$^{-/-}$* mice.

Adenosine and AR levels in the lungs of ADA/A$_1$AR double-knockout mice. Many of the pulmonary phenotypes seen in *ADA$^{-/-}$* mice have been attributed to elevations in lung-adenosine concentrations (11, 31, 34). Lung-adenosine levels were monitored to determine whether exaggerated pulmonary phenotypes in *ADA/A$_1$AR* double-knockout mice were associated with increased adenosine concentrations. The lungs of *ADA$^{-/-}$* mice containing the *A$_1$AR* exhibited an approximately 10-fold increase in adenosine levels as compared to *ADA$^+$* controls whereas lung adenosine levels were increased 20-fold in the lungs of *ADA/A$_1$AR* double-knockout mice (Figure 7A). The augmented accumulation of adenosine in the lungs of *ADA/A$_1$AR* double-knockout mice is consistent with enhanced tissue inflammation and damage in this model.

Next, lung *AR* transcript levels were examined to determine if there were compensatory effects on AR expression in the absence of the *A$_1$AR*. Transcript levels for the A$_1$AR, A$_{2B}$AR, and A$_3$AR were found to increase in whole-lung RNA extracts from *ADA$^{-/-}$* mice while levels of the A$_{2A}$AR decreased (Figure 7B). However, there were no differences in lung *AR* transcript levels between *ADA$^+$* and *ADA$^{-/-}$* mice with or without the *A$_1$AR* except for the *A$_1$AR* transcript that was not detected in *A$_1$AR$^{-/-}$* mice (Figure 7B). These

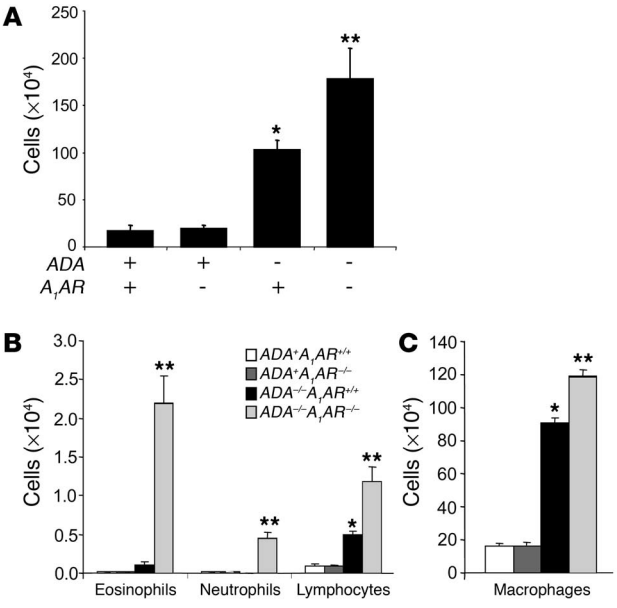

Figure 3
Increased airway inflammation in *ADA/A$_1$AR* double-knockout mice. BALF was collected from the lungs of postnatal day 14 mice, and total cells were determined (**A**). BALF cells were then cytospun and stained with Diff-Quick (Dade Behring), allowing for determination of cellular differentials. Cells examined in BALF included eosinophils, neutrophils, and lymphocytes (**B**) as well as alveolar macrophages (**C**). All data are presented as total cells ± SEM; $n = 10$ for each group. $^*P \le 0.05$ compared to *ADA$^+$* mice; $^{**}P \le 0.05$ compared to *ADA$^{-/-}$A$_1$AR$^{+/+}$* mice.

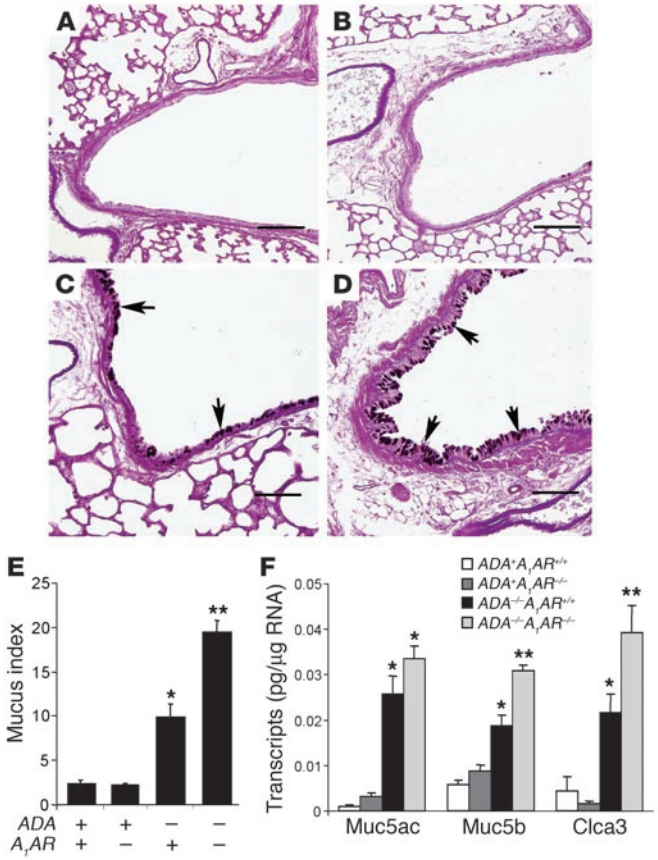

Figure 4
Increased mucus production in the lungs of *ADA/A$_1$AR* double-knockout mice. Lung sections from postnatal day 14 mice were stained with PAS for the detection of mucus (arrows). Images show (**A**) lung from an *ADA$^+$A$_1$AR$^{+/+}$* mouse, (**B**) lung from an *ADA$^+$A$_1$AR$^{-/-}$* mouse, (**C**) lung from an *ADA$^{-/-}$A$_1$AR$^{+/+}$* mouse, and (**D**) lung from an *ADA$^{-/-}$A$_1$AR$^{-/-}$* mouse. Scale bar: 100 μm. (**E**) A mean mucus index ± SEM was determined as described in Methods; $n = 5$ for each group. (**F**) Levels of mucus-associated genes were determined in whole-lung extracts from postnatal day 14 mice, using quantitative RT-PCR. Data are presented as mean pg of transcripts/μg RNA ± SEM; $n = 8$ for each group. *$P \leq 0.05$ compared to *ADA$^+$* mice; **$P \leq 0.05$ compared to *ADA$^{-/-}$A$_1$AR$^{+/+}$* mice.

findings demonstrate that there are no compensatory changes in the levels of *A$_{2A}$AR*, *A$_{2B}$AR*, and *A$_3$AR* transcripts in the lungs following the removal of the *A$_1$AR*.

Alveolar destruction in the lungs of ADA/A$_1$ double-knockout mice. The alveolar airways of *ADA$^{-/-}$* mice were substantially enlarged on postnatal day 14 (Figure 2C), suggesting the activation of proteolytic pathways that can cause emphysemic changes. However, previous studies have demonstrated that defects in alveolar development contribute to the enlarged alveoli seen in *ADA$^{-/-}$* mice (11, 35). Therefore, in order to assess the contribution of the *A$_1$AR* to the alveolar destruction seen in *ADA$^{-/-}$* mice, *ADA$^{-/-}$* mice with or without the *A$_1$AR* were maintained on ADA enzyme therapy from birth to allow for normal alveolar development to occur (36). Mice were maintained on ADA enzyme therapy for the first 17 days of life; then therapy was discontinued and pulmonary endpoints were examined 14 days later. Examination of adenosine levels from mice treated in this manner demonstrated that lung adenosine levels are not elevated in the lungs of *ADA$^{-/-}$* mice 3 days after the cessation of ADA enzyme therapy but are markedly elevated 14 days after treatment (Figure 8). Examination of pulmonary endpoints 14 days after the cessation of ADA enzyme therapy revealed similar inflammatory changes, increased mucus production, and elevations in cytokines and chemokines as seen in *ADA$^{-/-}$* mice on postnatal day 14 (data not shown). Moreover, enhanced inflammation, mucus production, and cytokine and chemokine elaboration were seen in *ADA$^{-/-}$* mice lacking the *A$_1$AR* (data not shown). Analysis of alveolar destruction in *ADA$^{-/-}$* mice 14 days after the cessation of ADA enzyme therapy demonstrated a significant increase in alveolar size (Figure 9, C and E). The degree of airway enlargement was substantially increased in the lungs of *ADA$^{-/-}$* mice lacking the *A$_1$AR* (Figure 9, D and E). We next examined the expression of key proteolytic mediators in the lungs of these mice. Expression of MMP-9 was elevated in the lungs of *ADA$^{-/-}$* mice with and without the *A$_1$AR* (Figure 9F), whereas expression of MMP-12 was not elevated in the lungs of *ADA$^{-/-}$* mice containing the *A$_1$AR* but was markedly increased in the lungs of *ADA/A$_1$AR* double-knockout mice. These findings demonstrate that there is increased MMP-12 expression and alveolar destruction in the lungs of *ADA/A$_1$AR* double-knockout mice.

Discussion

Removal of ADA from mice has created a model system for examining the physiological consequences of adenosine elevations (32). *ADA$^{-/-}$* mice develop progressive pulmonary inflammation and airway remodeling in association with elevations in adenosine levels. Preventing or reversing the levels of adenosine in the lungs of these mice using ADA enzyme therapy can prevent or reverse aspects of pulmonary inflammation and damage seen (11, 31, 36). These findings suggest that adenosine is serving a proinflammatory role in the development of pulmonary injury. This is consistent with the proposed roles for adenosine in the development and progression of lung diseases such as asthma and COPD (5, 6, 37). The mechanisms by which adenosine elicits its functions in the inflamed lung are not well understood. Our approach to investigating the impact of adenosine on lung injury has been to examine the role of specific ARs in the adenosine-mediated pul-

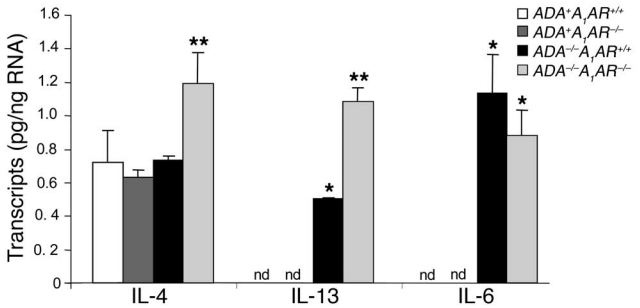

Figure 5
Cytokine transcript levels in the lungs of *ADA/A$_1$AR* double-knockout mice. Levels of *IL-4*, *IL-13*, and *IL-6* transcripts were determined in whole-lung extracts from postnatal day 14 mice using quantitative RT-PCR. Data are presented as mean pg of transcripts/μg RNA ± SEM; $n = 8$ for each. *$P \leq 0.05$ compared to *ADA$^+$* mice; **$P \leq 0.05$ compared to ADA$^{-/-}$A$_1$AR$^{+/+}$ mice.

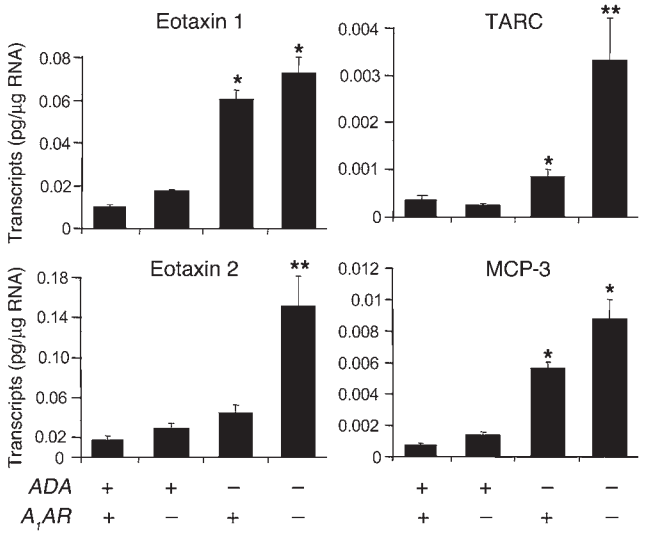

Figure 6
Chemokine transcript levels in the lungs of *ADA*/*A*$_1$*AR* double-knockout mice. Levels of *eotaxin 1*, *eotaxin 2*, *TARC*, and *MCP-3* transcripts were determined in whole-lung extracts from postnatal day 14 mice using quantitative RT-PCR. Data are presented as mean pg of transcripts/μg RNA ± SEM; $n = 8$ for each. *$P \le 0.05$ compared to *ADA*$^+$ mice; **$P \le 0.05$ compared to *ADA*$^{-/-}$*A*$_1$*AR*$^{+/+}$ mice.

monary phenotypes seen in *ADA*$^{-/-}$ mice. In the current study, we examined the role of the A_1AR in this model and found that the genetic removal of the *A*$_1$*AR* resulted in enhanced pulmonary inflammation, mucus metaplasia, alveolar destruction. and precocious death of *ADA*$^{-/-}$ mice, suggesting that A_1AR receptor signaling may play an anti-inflammatory and/or tissue protective role in the progression of pulmonary disease. These findings provide what we believe to be the first evidence that the *A*$_1$*AR* is playing a protective role in a model in which endogenous adenosine levels are elevated and suggest that there is a complex interplay between anti- and proinflammatory adenosine-mediated pathways in the progression and maintenance of chronic lung disease.

At first glance, it may appear that a paradox exists between previous findings demonstrating that lowering adenosine levels can decrease pulmonary inflammation and injury in *ADA*$^{-/-}$ mice (11) and the current findings demonstrating that A_1AR signaling plays an anti-inflammatory/protective role in this same model. However, it must be considered that all 4 of the ARs are expressed in the lungs of *ADA*$^{-/-}$ mice (31) and that receptor-specific activities that affect the overall balance of inflammation and structural changes seen in the lung likely exist on various cell types. For example, a recent study from our laboratory demonstrated that removal of the *A*$_3$*AR* from *ADA*$^{-/-}$ mice results in decreased airway inflammation, suggesting a proinflammatory role for A_3AR signaling in this model (33). Thus, different ARs elicit different functions in the lungs of *ADA*$^{-/-}$ mice in which adenosine levels are elevated. Furthermore, adenosine is generated in response to cell stress and damage, and its levels in the airways correlate with the degree of inflammation seen (4). Consistent with this, we found that adenosine levels were hyperelevated in *ADA*$^{-/-}$ mice that lack the *A*$_1$*AR* and exhibit increased pulmonary inflammation and injury. These hyperelevations in adenosine may in turn lead to increased activation of proinflammatory and injury pathways accessed by other ARs. Therefore, increased inflammation and subsequent enhanced adenosine elevations may serve as an amplification pathway that can perpetuate pulmonary injury in this model. Determining the cellular localization and function of all the ARs in the lungs of *ADA*$^{-/-}$ mice will provide interesting information into how these receptors work in concert to regulate pulmonary inflammation and injury.

Whereas the marked increase in pulmonary inflammation and injury seen in *ADA*$^{-/-}$/*A*$_1$*AR*$^{-/-}$ mice clearly suggests an anti-inflammatory or protective role for the A_1AR receptor in this model, it is less clear whether this implies clinical benefit from the use of A_1AR agonist in the treatment of pulmonary disorders. The A_1AR has a high affinity for adenosine, and adenosine levels are elevated in the lungs of asthmatics (3, 4). It is therefore unlikely that the addition of an A_1AR agonist would be effective. However, it is not known whether adenosine levels are chronically elevated in the lungs of asthmatic and COPD patients or whether they are elevated as a result of acute exacerbations. If the latter is the case, then utility of A_1AR agonism may exist. Additional studies are needed to characterize the levels of adenosine present in the airways of asthma and COPD patients at various stages during the progression of these disorders. This information will provide valuable insight into the design of specific AR

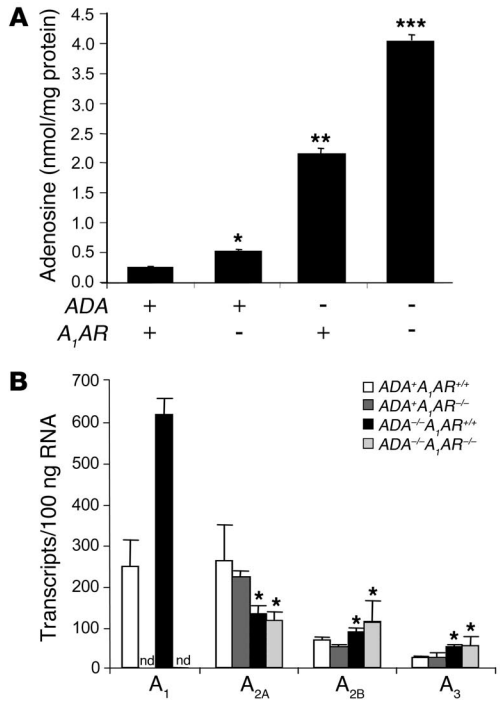

Figure 7
Adenosine and AR levels in the lungs of *ADA*/*A*$_1$*AR* double-knockout mice. (**A**) Adenosine levels were measured in the lungs of postnatal day 17 mice using reversed phase HPLC. Data are presented as mean nmol adenosine/mg protein ± SEM; $n = 8$ for each group. *$P \le 0.05$ compared to *ADA*$^+$*ADA*$^{+/+}$ mice; **$P \le 0.05$ compared to *ADA*$^+$ mice; ***$P \le 0.05$ compared to *ADA*$^{-/-}$*A*$_1$*AR*$^{+/+}$ mice. (**B**) Levels of *AR* transcripts were determined in whole-lung extracts from postnatal day 14 mice using quantitative RT-PCR. Data are presented as mean transcripts/100 ng RNA ± SEM; $n = 6$ for each. *$P \le 0.05$ compared to *ADA*$^+$ mice.

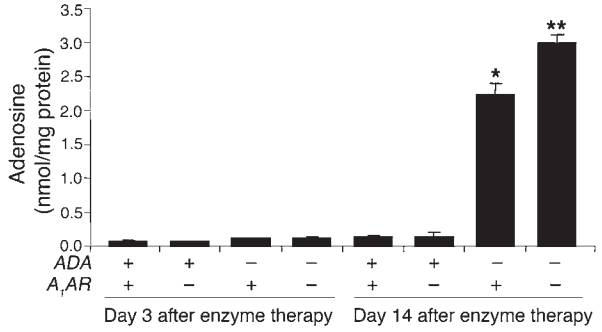

Figure 8
Regulation of lung adenosine levels using ADA enzyme therapy. *ADA*$^{-/-}$ mice were maintained on ADA enzyme therapy until postnatal day 17 as described in Methods. Whole-lung adenosine levels were measured in mice at 3 and 14 days after the cessation of ADA enzyme therapy. Data are presented as mean nmol adenosine/mg protein ± SEM; day 3, $n = 4$; day 14, $n = 7$. *$P \leq 0.05$ compared to *ADA*$^{+}$ mice; **$P \leq 0.05$ compared to *ADA*$^{-/-}$*A*$_1$*AR*$^{+/+}$ mice.

agonists and antagonists for the treatment of selective attributes of chronic lung diseases such as asthma and COPD.

Anti-inflammatory and tissue-protective effects of the A_1AR in the lungs of *ADA*$^{-/-}$ mice are consistent with findings in other model systems utilizing *A*$_1$*AR*$^{-/-}$ mice. In a model of renal ischemia and reperfusion injury, *A*$_1$*AR*$^{-/-}$ mice were found to exhibit increased production of proinflammatory mediators and increased renal injury (23, 24). Similarly, *A*$_1$*AR*$^{-/-}$ mice were reported to exhibit increased neuroinflammation and worsened demyelination and axonal injury in a model of allergic encephalomyelitis (21). Both studies concluded that the A_1AR serves anti-inflammatory functions that regulate subsequent tissue damage. Based on our findings, we propose an analogous role for A_1AR signaling in the regulation of pulmonary phenotypes in *ADA*$^{-/-}$ mice. However, an anti-inflammatory or tissue-protective role for A_1AR signaling is not consistent with observations using pharmacologic approaches to examine A_1AR signaling in the lung. Treatment with A_1AR antagonists have been shown to be beneficial in attenuating ischemia reperfusion (28) and endotoxin-induced (29) lung injury, suggesting a proinflammatory role for A_1AR signaling in acute lung injury. In addition, A_1AR activation has been implicated in the regulation of bronchoconstriction in allergic rabbit models (25–27), suggesting a provocative role for A_1AR signaling in acute phases of asthma.

The differences in the attributed functions of the A_1AR are likely related to differences in the model systems used, the endpoints examined, or the reliability of the pharmacological agents used. Additional studies are needed examining pulmonary endpoints in *A*$_1$*AR*$^{-/-}$ mice subjected to ischemia reperfusion and endotoxin injury models as well as allergen sensitization and challenge protocols.

Removal of the A_1AR resulted in elevations in proinflammatory mediators in the lungs of *ADA*$^{-/-}$ mice. There was a marked increase in the levels of IL-13, which is a pluripotent cytokine that can access numerous signaling pathways associated with pulmonary inflammation and chronic airway remodeling (38–40). In addition, IL-4, which is not elevated in the lungs of *ADA*$^{-/-}$ mice (11), was increased in the lungs of *ADA/A*$_1$*AR* double-knockout mice. Thus, removal of A_1AR-receptor signaling promotes the production of Th2 cytokines in an adenosine-rich environment. The mechanisms by which adenosine is regulating the levels of IL-13 and IL-4 are not known but may relate to the regulation of intracellular cAMP levels. Increased IL-4 and IL-13 production is associated with elevations in cAMP (41–43), and recent findings have demonstrated that adenosine can promote the expression of IL-4 and IL-13 in mast cells by engaging the A_{2B}AR (44), which couples to $G_{\alpha s}$ to activate adenylate cyclase and elevate cAMP (15). The A_{2B}AR has relatively low affinity for adenosine. Thus, in situations in which adenosine levels are elevated, A_{2B}AR engagement may serve to elevate the expression of IL-13 and/or IL-4. The A_1AR couples to $G_{\alpha i}$, which inhibits adenylate cyclase to lower cAMP (15). Engagement of this receptor may serve to dampen the levels of IL-13 and IL-4 produced in cells. Based on this model, as inflammation and damage increase in the lung and adenosine levels rise, A_{2B}AR-mediated effects would predominate over the anti-

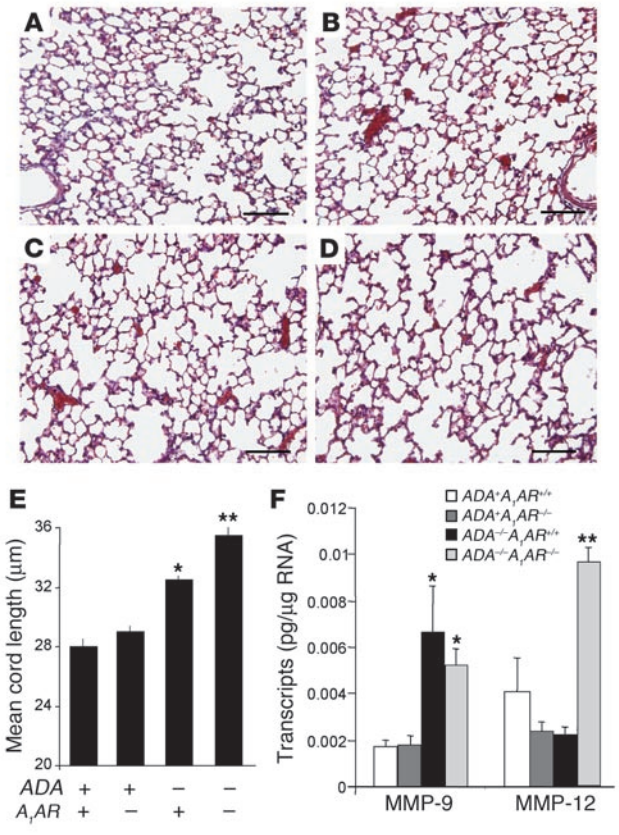

Figure 9
Alveolar destruction in *ADA/A*$_1$*AR* double-knockout mice. *ADA*$^{-/-}$ mice were treated with ADA enzyme therapy from birth until postnatal day 14 as described in Methods. Lungs from *ADA*$^{-/-}$ mice and age-matched *ADA*$^{+}$ mice were collected 14 days after the cessation of ADA enzyme therapy and processed for H&E staining. Images show (**A**) lung from an *ADA*$^{+}$*A*$_1$*AR*$^{+/+}$ mouse, (**B**) lung from an *ADA*$^{+}$*A*$_1$*AR*$^{-/-}$ mouse, (**C**) lung from an *ADA*$^{-/-}$*A*$_1$*AR*$^{+/+}$ mouse, and (**D**) lung from an *ADA*$^{-/-}$*A*$_1$*AR*$^{-/-}$ mouse. Images are representative of 10 animals from each group. Scale bar: 100 μm. (**E**) Alveolar airway sizes were calculated using Image-Pro Plus (Media Cybernetics). Data are presented as mean cord length ± SEM; $n = 5$. (**F**) Levels of *MMP-9* and *MMP-12* transcripts were determined in whole-lung extracts from postnatal day 14 mice using quantitative RT-PCR. Data are presented as mean pg of transcripts/μg RNA ± SEM; $n = 8$ for each. *$P \leq 0.05$ compared to *ADA*$^{+}$ mice; **$P \leq 0.05$ compared to *ADA*$^{-/-}$*A*$_1$*AR*$^{+/+}$ mice.

inflammatory effects of A_1AR signaling and thus contribute to the promotion of chronic lung injury. Previous studies in *ADA*$^{-/-}$ mice and in IL-13 transgenic mice have implicated adenosine and IL-13 as being in an amplification loop that serves to promote aspects of chronic lung disease (12). Hyperelevations of IL-13 in the lungs of *ADA/A1AR* double-knockout mice in which there are hyperelevations in adenosine are consistent with this hypothesis. Current investigations are focusing on determining the specific cell types that produced IL-13 in the lungs of *ADA*$^{-/-}$ mice and examining the role of A_{2B}AR signaling in these processes.

There was a significant increase in alveolar airway size in the lungs of *ADA/A1AR* double-knockout mice. Associated with these emphysemic changes was an increase in MMP-12 expression. MMP-12, also known as macrophage elastase, is a matrix metalloproteinase that is produced by activated macrophages and preferentially degrades elastin (45, 46). MMP-12 has been shown to account for emphysemic changes in the lungs of mice in response to a number of stimuli (47–49), and MMP-12 levels are elevated in patients with emphysema, where MMP-12 is believed to play a major role in the progressive loss of alveolar structure (50, 51). We detected A_1AR expression in alveolar macrophages in *ADA*$^{-/-}$ mice but not in *ADA*$^{+}$ mice (Figure 1), suggesting an upregulation of this receptor on activated alveolar macrophages. Our data suggest that A_1AR signaling in alveolar macrophages may serve to dampen MMP-12 expression in the lungs of *ADA*$^{-/-}$ mice and in so doing slow the progression of alveolar destruction. Consistent with this concept, recent studies have demonstrated that macrophages and microglia cells from *A1AR*$^{-/-}$ mice exhibit increased expression of MMP-12 when challenged with inflammatory stimuli (21). Adenosine does not appear to directly regulate MMP-12 expression in macrophages since direct stimulation of cultured alveolar macrophages with AR agonists did not induce expression of MMP-12 (data not shown). It is therefore likely that the removal of A_1AR signaling leads to enhanced production of mediators in the lungs, which then leads to enhanced MMP-12 production. A likely candidate for this is IL-13. IL-13 has been shown to be involved in the production of MMP-12 in other model systems (49, 52), and we demonstrate that IL-13 levels are hyperelevated in the lungs of *ADA/A1AR* double-knockout mice (Figure 5). In further support of this model, we have previously shown that regulating lung adenosine levels in vivo can also regulate the production of IL-13 (12), suggesting that adenosine signaling may drive the production of IL-13. Increases in adenosine likely lead to increased IL-13 production, which in turn leads to enhanced MMP-12 production. Another pathway recently implicated in MMP-12 regulation in the lung is the TGF-β1–signaling pathway. Studies have demonstrated that disruption of TGF-β1 signaling is associated with increased production of MMP-12 and increased alveolar simplification in the lungs (48, 53). Thus, it is possible that removal of A_1AR signaling may perturb normal TGF-β1 signaling, which may in turn have an impact on MMP-12 expression. In addition, it must be noted that other matrix metalloproteinases, such as MMP-9, are expressed in the lungs of *ADA*$^{-/-}$ mice in a manner independent of A_1AR expression (Figure 9F), suggesting that other unidentified signaling pathways related to adenosine elevations are involved in alveolar simplification seen in the lungs of *ADA/A1AR* double-knockout mice.

Persistent inflammation and progressive airway remodeling and alveolar destruction are features of chronic lung diseases such as asthma and/or COPD (1, 2). The production of adenosine in the lungs of asthmatics is not surprising given the degree of inflammation and damage that occurs in this disease. However, deciphering the functions of this potent signaling nucleoside in the development and maintenance of lung inflammation and injury has proven difficult, given the diverse roles of ARs on various cell types. The *ADA*$^{-/-}$ mouse model is an appropriate model of a situation in which elevations in lung adenosine lead to the development of inflammatory and structural changes that resemble those seen in certain patients with severe asthma and COPD. Results from this study demonstrate that the A_1AR plays an anti-inflammatory and tissue-protective role in the development of pulmonary inflammation and injury in *ADA*$^{-/-}$ mice. It will be important to examine the interplay of AR signaling in other model systems as well as in the lungs of individuals with chronic lung disease in order to determine how these pathways can be manipulated to ultimately treat the progression of asthma and COPD.

Methods

Mice. ADA-deficient mice were generated and genotyped as described (33, 54). Mice homozygous for the null *Ada* allele were designated ADA-deficient (*ADA*$^{-/-}$) while mice heterozygous for the null *Ada* allele were designated as ADA control mice (*ADA*$^{+}$). ADA/A_1AR double-knockout mice were generated by mating *ADA*$^{-/-}$ mice with A_1AR-deficient mice (*A1AR*$^{-/-}$) (55). The following primers were used to track *A1AR* alleles: wild-type sense primer, 5′- GTACATCTCGGCCTTCCAGG-3′; wild-type antisense primer, 5′-GAGAATACCTGGCTGACTAG-3′; mutant-sense primer, 5′- TTCACTGGCCGTCGTTTTACAACGTCGTGA-3′; mutant-antisense primer, 5′-ATGTGAGCGAGTAACAACCCGTCGGATTCT-3′. All mice were on a mixed 129sv/C57BL/6J background, and all phenotypic comparisons were performed among littermates. All experiments were repeated at least 3 times. Animal care was in accordance with the Animal Care Committee at the University of Texas Health Science Center at Houston and NIH guidelines. All mice were housed in ventilated cages equipped with microisolator lids and maintained under strict containment protocols. No evidence of bacterial, parasitic, or fungal infection was found, and serologies on cage littermates were negative for 12 of the most common murine viruses.

ADA enzyme therapy. Polyethylene glycol modified–ADA (PEG-ADA) was generated by the covalent modification of purified bovine ADA with activated polyethylene glycol as described previously (33). *ADA*$^{-/-}$ mice received intramuscular injections of PEG-ADA on postnatal days 1, 5, 9, 13, and 17 (0.625, 1.25, 2.5, 2.5, and 2.5 units, respectively). All mice were sacrificed on day 14 after the last PEG-ADA injection.

Bronchial alveolar lavage. Mice were anesthetized with avertin, and lungs were lavaged 4 times with 0.3 ml PBS; 0.95–1 ml of pooled lavage fluid was recovered. Total cell counts were determined using a hemocytometer, and aliquots were cytospun onto microscope slides and stained with Diff-Quick (Dade Behring) for cellular differentials.

Histology. Aged-matched control and experimental animals were sacrificed, and the lungs were infused with 4% paraformaldehyde in PBS at 25 cm of pressure and then fixed overnight at 4°C. Fixed lung samples were rinsed in PBS, dehydrated, and embedded in paraffin. Sections (5 μm) were collected on microscope slides and stained with H&E (Shandon-Lipshaw) or PAS (EM Science) according to manufacturer's instructions.

Mucus index. The extent of mucus production in bronchial airways was determined by quantifying the amount of PAS-stained material in the bronchial airways using Image-Pro Plus analysis software (Media Cybernetics) (11). PAS-stained material was identified on digitized images, and the pixel intensities of each color channel (red, blue, and green) were averaged. This was repeated for each image, and the values were averaged and used to deter-

Table 1
Quantitative RT-PCR primers

Genes of interest		Primer sequences
Muc5ac	Sense	5′-GGACCAAGTGGTTTGACACTGAC-3′
	Antisense	5′-CCTCATAGTTGAGGCACATCCCAG-3′
Muc5b	Sense	5′-ATCCGCCTAGTCCTCACCTT-3′
	Antisense	5′-CATCCTGGCACTGCTCTGTA-3′
mCLCA3	Sense	5′-CATCCGAATGAGCACCAGTA-3′
	Antisense	5′-CACAGCCTGGATAGCAATGA-3′
IL-4	Sense	5′-TCCTCACAGCAACGAAGAAC-3′
	Antisense	5′-TGCAGCTCCATGAGAACACT-3′
IL-5	Sense	5′-TCCTGAAGGCTGAGGTTACA-3′
	Antisense	5′-GATGCAACGAAGAGGATGAG-3′
IL-6	Sense	5′-TCCTCTGGTCTTCTGGAGTA-3′
	Antisense	5′-CTTAGCCACTCCTTCTGTGA-3′
IL-9	Sense	5′-GATTGTACCACACCGTGCTA-3′
	Antisense	5′-GACGGACACGTGATGTTCTT-3′
IL-13	Sense	5′-AGACCAGACTCCCCTGTGCA-3′
	Antisense	5′-TGGGTCCTGTAGATGGCATTG-3′
IL-17	Sense	5′-GTGAAGGCAGCAGCGATCAT-3′
	Antisense	5′-TGACGTGGAACGGTTGAGGT-3′
Eotaxin 1	Sense	5′-CTTCTATTCCTGCTGCTCAC-3′
	Antisense	5′-CCAACCTGGTCTTGAAGACT-3′
Eotaxin 2	Sense	5′-GTGGCAATAGCACCGAGGTT-3′
	Antisense	5′-CATGCTTGCAGCTCACTCAG-3′
MCP-3	Sense	5′-GCTGCTCATAGCCGCTGCTT-3′
	Antisense	5′-TCAGCGCAGACTTCCATGCC-3′
TARC	Sense	5′-AGAAGGCCATCAGATTGGTG-3′
	Antisense	5′-TGTGTTCGCCTGTAGTGCAT-3′
TNF-α	Sense	5′-CACCACCATCAAGGACTCAA-3′
	Antisense	5′-TCCAGCCTCATTCTGAGACA-3′
TGF-β	Sense	5′-CTTCAGCTCCACAGAGAAGA-3′
	Antisense	5′-GACAGAAGTTGGCATGGTAG-3′
IFN-γ	Sense	5′-CCAAGCGGCTGACTGAACTC-3′
	Antisense	5′-AGTGCTGTCTGGCCTGCTGT-3′
RANTES	Sense	5′-TCGAAGGAACCGCCAAGTGT-3′
	Antisense	5′-CCAAGCTGGCTAGGACTAGA-3′
CCR3	Sense	5′-TCTTCCTCTCCTCGTTATGG-3′
	Antisense	5′-TAGGCAATCACCTCAGTCAC-3′
MMP-9	Sense	5′-AGTGGACGCGACCGTAGTTG-3′
	Antisense	5′-GCCACCAGGAACAGGCTGTA-3′
MMP-12	Sense	5′-GAGTCCAGCCACCAACATTA-3′
	Antisense	5′-TCCTGCCTCACATCATACCT-3′

mine the area (*M*) and intensity (*I*) of PAS-stained material in bronchial airways. In addition, the area (*A*) of the total epithelium (including PAS-stained material) was determined. The mucus index was determined using the following formula: $M \times I/A$. Final indices were results of an average of 10 images per lung encompassing large and small bronchial airways. All quantitative studies were performed blind with regard to animal genotype.

Airway size measurement. The size of alveolar airways was determined in pressure-infused lungs by measuring mean cord lengths on H&E-stained lung sections (11). Representative images were digitized, and a grid consisting of 53 black lines at 10.5-μm intervals was overlaid on the image. This line grid was subtracted from the lung images using Image-Pro Plus image analysis software (Media Cybernetics), and the resultant lines were measured and averaged to determine the mean cord length of the alveolar airways. The final mean cord lengths represent averages from 10 nonoverlapping images of each lung specimen. All quantitative studies were performed blinded with regards to animal genotype.

RT-PCR and quantitative RT-PCR. Total RNA was isolated from whole-lung tissue using Trizol reagent (Invitrogen Corp.). Total RNA was treated using RNase-free DNase (Invitrogen Corp.). Lung RNA (1 μg) was used in a Superscript One-Step RT-PCR (Invitrogen Corp.) reaction with A_1AR- or β-actin–specific primers following manufacturer's instructions. Alternatively, transcript levels were quantified using real-time quantitative RT-PCR. AR and β-actin transcripts were analyzed using Taqman probes on the Smart Cycler (Cepheid) (31). Specific quantitative primers for mediators were developed using Primer Express software (PE Applied Biosystems) following the recommended guidelines based on sequences from GenBank (Table 1). Transcripts levels were determined by SYBR green analysis using a Smart Cycler (Cepheid). PCR conditions and product confirmation were as described previously (33).

In situ hybridization. The cDNA encoding full-length mouse A_1AR cDNA (56) was subcloned into pBluescript II (+). The plasmid was linearized using *Xba* I (sense) or *Acc* I (antisense) and subsequently served as a template to synthesize the digoxigenin-labeled (DIG-labeled) riboprobes (sense, T3 RNA polymerase; antisense, T7 RNA polymerase) with a DIG RNA Labeling Kit (Roche Diagnostics). Probes were analyzed on 3% acrylamide gel to determine quality and relative quantity. Paraffin tissue sections (5 μm) were dewaxed, rehydrated, rinsed in TBS (50 mM Tris-HCl, pH 7.5; 150 mM NaCl), fixed at 4% paraformaldehyde buffer (PFA) for 15 minutes, permeabilized with 0.1% Trition X-100 for 10 minutes at room temperature, rinsed with TBS, and then denatured with 200 mM HCl for 10 minutes at room temperature. Sections were postfixed with 4% PFA and then treated with 0.5% acetic anhydride in Tris-HCl (pH 8.0). Following dehydration, hybridization was performed at 60°C overnight in a solution containing 50% deionized formamide, 2 × SSC, and 10% dextran sulphate, 0.02% SDS, and labeled cRNA probe. Sections were washed with 50% formamide in 2 × SSC at 60°C followed by 30 minutes with 1 × SSC. Sections were then incubated with 10% goat serum in TBS for 30 minutes at room temperature, and this was followed by incubation with a sheep alkaline phosphatase–conjugated polyclonal antibody $F(ab)_2$ fragment against DIG (1:500) (Roche Diagnostics) for 4 hours at room temperature. Signal was detected using 5-bromo-4-chloro-3-indolyl phosphate (NCIP) as a substrate and nitroblue tetrazolium (NBT) as a coupler (Roche Diagnostics), and sections were counterstained using Nuclear Fast Red (Vector Laboratories).

Quantification of adenosine. Mice were anesthetized, the thoracic cavity exposed, and the lungs rapidly removed and frozen in liquid nitrogen. Adenine nucleosides were extracted from frozen lungs using 0.4 N perchloric acid as described (57), and adenosine was quantified using reversed-phase HPLC (57). Adenosine levels were normalized to protein content, and values are given as nmol/mg protein.

Statistical analysis. Analysis of variance was used to determine the level of difference among all groups. Single pairs of groups were compared using the Student's *t* test. *P* values for significance were set at 0.05.

Acknowledgments

This work was supported by NIH grants AI-43572 and HL-70952 (to M.R. Blackburn).

Received for publication July 7, 2004, and accepted in revised form November 2, 2004.

Address correspondence to: Michael R. Blackburn, Department of Biochemistry and Molecular Biology, The University of Texas Health Science Center at Houston Medical School, 6431 Fannin Street, Houston, Texas 77030, USA. Phone: (713) 500-6087; Fax: (713) 500-0652; E-mail: michael.r.blackburn@uth.tmc.edu.

1. Elias, J.A., et al. 2003. New insights into the pathogenesis of asthma. *J. Clin. Invest.* **111**:291–297. doi:10.1172/JCI200317748.
2. Senior, R.M., and Shapiro, S.D. 1998. Chronic obstructive pulmonary disease: Epidemiology, pathophysiology, and pathogenesis. In *Fishman's pulmonary diseases and disorders*. 3rd edition. A.P. Fishman, et al., editors. McGraw-Hill, Inc. New York, New York, USA. 659–681.
3. Driver, A.G., Kukoly, C.A., Ali, S., and Mustafa, S.J. 1993. Adenosine in bronchoalveolar lavage fluid in asthma. *Am. Rev. Respir. Dis.* **148**:91–97.
4. Huszar, E., et al. 2002. Adenosine in exhaled breath condensate in healthy volunteers and in patients with asthma. *Eur. Respir. J.* **20**:1393–1398.
5. Jacobson, M.A., and Bai, T.R. 1997. The role of adenosine in asthma. In *Purinergic approaches in experimental therapeutics*. K.A. Jacobson and M.F. Jarvis, editors. Wiley-Liss. New York, New York, USA. 315–331.
6. Fozard, J.R., and Hannon, J.P. 1999. Adenosine receptor ligands: potential as therapeutic agents in asthma and COPD. *Pulm. Pharmacol. Ther.* **12**:111–114.
7. Cushley, M.J., Tattersfield, A.E., and Holgate, S.T. 1983. Inhaled adenosine and guanosine on airway resistance in normal and asthmatic subjects. *Br. J. Clin. Pharmacol.* **15**:161–165.
8. Oosterhoff, Y., de Jong, J.W., Jansen, M.A., Koeter, G.H., and Postma, D.S. 1993. Airway responsiveness to adenosine 5′-monophosphate in chronic obstructive pulmonary disease is determined by smoking. *Am. Rev. Respir. Dis.* **147**:553–558.
9. Richards, R., Phillips, G.D., and Holgate, S.T. 1989. Nedocromil sodium is more potent than sodium cromoglycate against AMP-induced bronchoconstriction in atopic asthmatic subjects. *Clin. Exp. Allergy.* **19**:285–291.
10. Cushley, M.J., and Holgate, S.T. 1985. Adenosine-induced bronchoconstriction in asthma: role of mast cell-mediator release. *J. Allergy Clin. Immunol.* **75**:272–278.
11. Blackburn, M.R., et al. 2000. Metabolic consequences of adenosine deaminase deficiency in mice are associated with defects in alveogenesis, pulmonary inflammation, and airway obstruction. *J. Exp. Med.* **192**:159–170.
12. Blackburn, M.R., et al. 2003. Adenosine mediates IL-13–induced inflammation and remodeling in the lung: evidence for an IL-13–adenosine amplification pathway. *J. Clin. Invest.* **112**:332–344. doi:10.1172/JCI200316815.
13. Linden, J. 2001. Molecular approach to adenosine receptors: receptor-mediated mechanisms of tissue protection. *Annu. Rev. Pharmacol. Toxicol.* **41**:775–787.
14. Hasko, G., and Cronstein, B.N. 2004. Adenosine: an endogenous regulator of innate immunity. *Trends Immunol.* **25**:33–39.
15. Fredholm, B.B., Ijzerman, A.P., Jacobson, K.A., Klotz, K.N., and Linden, J. 2001. International Union of Pharmacology. XXV. Nomenclature and classification of adenosine receptors. *Pharmacol. Rev.* **53**:527–552.
16. Khoa, N.D., et al. 2001. Inflammatory cytokines regulate function and expression of adenosine A(2A) receptors in human monocytic THP-1 cells. *J. Immunol.* **167**:4026–4032.
17. Xaus, J., et al. 1999. IFN-gamma up-regulates the A2B adenosine receptor expression in macrophages: a mechanism of macrophage deactivation. *J. Immunol.* **162**:3607–3614.
18. Salmon, J.E., and Cronstein, B.N. 1990. Fc gamma receptor-mediated functions in neutrophils are modulated by adenosine receptor occupancy. A1 receptors are stimulatory and A2 receptors are inhibitory. *J. Immunol.* **145**:2235–2240.
19. Salmon, J.E., et al. 1993. Human mononuclear phagocytes express adenosine A1 receptors. A novel mechanism for differential regulation of Fc gamma receptor function. *J. Immunol.* **151**:2775–2785.
20. Merrill, J.T., et al. 1997. Adenosine A1 receptor promotion of multinucleated giant cell formation by human monocytes: a mechanism for methotrexate-induced nodulosis in rheumatoid arthritis. *Arthritis Rheum.* **40**:1308–1315.
21. Tsutsui, S., et al. 2004. A1 adenosine receptor upregulation and activation attenuates neuroinflammation and demyelination in a model of multiple sclerosis. *J. Neurosci.* **24**:1521–1529.
22. Liao, Y., et al. 2003. Activation of adenosine A1 receptor attenuates cardiac hypertrophy and prevents heart failure in murine left ventricular pressure-overload model. *Circ. Res.* **93**:759–766.
23. Lee, H.T., Xu, H., Nasr, S.H., Schnermann, J., and Emala, C.W. 2004. A1 adenosine receptor knockout mice exhibit increased renal injury following ischemia and reperfusion. *Am. J. Physiol. Renal Physiol.* **286**:F298–F306.
24. Lee, H.T., Gallos, G., Nasr, S.H., and Emala, C.W. 2004. A1 adenosine receptor activation inhibits inflammation, necrosis, and apoptosis after renal ischemia-reperfusion injury in mice. *J. Am. Soc. Nephrol.* **15**:102–111.
25. Ali, S., Mustafa, S.J., and Metzger, W.J. 1994. Adenosine-induced bronchoconstriction and contraction of airway smooth muscle from allergic rabbits with late-phase airway obstruction: evidence for an inducible adenosine A1 receptor. *J. Pharmacol. Exp. Ther.* **268**:1328–1334.
26. el-Hashim, A., D'Agostino, B., Matera, M.G., and Page, C. 1996. Characterization of adenosine receptors involved in adenosine-induced bronchoconstriction in allergic rabbits. *Br. J. Pharmacol.* **119**:1262–1268.
27. Nyce, J.W., and Metzger, W.J. 1997. DNA antisense therapy for asthma in an animal model. *Nature.* **385**:721–725.
28. Neely, C.F., and Keith, I.M. 1995. A1 adenosine receptor antagonists block ischemia-reperfusion injury of the lung. *Am. J. Physiol.* **268**:L1036–L1046.
29. Neely, C.F., Jin, J., and Keith, I.M. 1997. A1-adenosine receptor antagonists block endotoxin-induced lung injury. *Am. J. Physiol.* **272**:L353–L361.
30. Zhong, H., Chunn, J.L., Volmer, J.B., Fozard, J.R., and Blackburn, M.R. 2001. Adenosine-mediated mast cell degranulation in adenosine deaminase-deficient mice. *J. Pharmacol. Exp. Ther.* **298**:433–440.
31. Chunn, J.L., Young, H.W., Banerjee, S.K., Colasurdo, G.N., and Blackburn, M.R. 2001. Adenosine-dependent airway inflammation and hyperresponsiveness in partially adenosine deaminase-deficient mice. *J. Immunol.* **167**:4676–4685.
32. Blackburn, M.R. 2003. Too much of a good thing: adenosine overload in adenosine-deaminase-deficient mice. *Trends Pharmacol. Sci.* **24**:66–70.
33. Young, H.W., et al. 2004. A3 adenosine receptor signaling contributes to airway inflammation and mucus production in adenosine deaminase-deficient mice. *J. Immunol.* **173**:1380–1389.
34. Banerjee, S.K., Young, H.W., Volmer, J.B., and Blackburn, M.R. 2002. Gene expression profiling in inflammatory airway disease associated with elevated adenosine. *Am. J. Physiol. Lung Cell Mol. Physiol.* **282**:L169–L182.
35. Banerjee, S.K., Young, H.W., Barczak, A., Erle, D.J., and Blackburn, M.R. 2004. Abnormal alveolar development associated with elevated adenine nucleosides. *Am. J. Physiol. Lung Cell Mol. Physiol.* **30**:38–50.
36. Blackburn, M.R., et al. 2000. The use of enzyme therapy to regulate the metabolic and phenotypic consequences of adenosine deaminase deficiency in mice. Differential impact on pulmonary and immunologic abnormalities. *J. Biol. Chem.* **275**:32114–32121.
37. Fozard, J.R. 2003. The case for a role for adenosine in asthma: almost convincing? *Curr. Opin. Pharmacol.* **3**:264–269.
38. Grunig, G., et al. 1998. Requirement for IL-13 independently of IL-4 in experimental asthma. *Science.* **282**:2261–2263.
39. Wills-Karp, M., et al. 1998. Interleukin-13: central mediator of allergic asthma. *Science.* **282**:2258–2260.
40. Zhu, Z., et al. 1999. Pulmonary expression of interleukin-13 causes inflammation, mucus hypersecretion, subepithelial fibrosis, physiologic abnormalities, and eotaxin production. *J. Clin. Invest.* **103**:779–788.
41. Tokoyoda, K., et al. 2004. Up-regulation of IL-4 production by the activated cAMP/cAMP-dependent protein kinase (protein kinase A) pathway in CD3/CD28-stimulated naive T cells. *Int. Immunol.* **16**:643–653.
42. Lacour, M., et al. 1994. cAMP up-regulates IL-4 and IL-5 production from activated CD4+ T cells while decreasing IL-2 release and NF-AT induction. *Int. Immunol.* **6**:1333–1343.
43. Chen, C.H., Zhang, D.H., LaPorte, J.M., and Ray, A. 2000. Cyclic AMP activates p38 mitogen-activated protein kinase in Th2 cells: phosphorylation of GATA-3 and stimulation of Th2 cytokine gene expression. *J. Immunol.* **165**:5597–5605.
44. Ryzhov, S., et al. 2004. Adenosine-activated mast cells induce IgE synthesis by B lymphocytes: an A2B-mediated process involving Th2 cytokines IL-4 and IL-13 with implications for asthma. *J. Immunol.* **172**:7726–7733.
45. Werb, Z., and Gordon, S. 1975. Elastase secretion by stimulated macrophages. Characterization and regulation. *J. Exp. Med.* **142**:361–377.
46. Shapiro, S.D., et al. 1992. Molecular cloning, chromosomal localization, and bacterial expression of a murine macrophage metalloelastase. *J. Biol. Chem.* **267**:4664–4671.
47. Hautamaki, R.D., Kobayashi, D.K., Senior, R.M., and Shapiro, S.D. 1997. Requirement for macrophage elastase for cigarette smoke-induced emphysema in mice. *Science.* **277**:2002–2004.
48. Morris, D.G., et al. 2003. Loss of integrin alpha(v)-beta6-mediated TGF-beta activation causes Mmp12-dependent emphysema. *Nature.* **422**:169–173.
49. Lanone, S., et al. 2002. Overlapping and enzyme-specific contributions of matrix metalloproteinases-9 and -12 in IL-13–induced inflammation and remodeling. *J. Clin. Invest.* **110**:463–474. doi:10.1172/JCI200214136.
50. Belaaouaj, A., et al. 1995. Human macrophage metalloelastase. Genomic organization, chromosomal location, gene linkage, and tissue-specific expression. *J. Biol. Chem.* **270**:14568–14575.
51. Shapiro, S.D. 1999. The macrophage in chronic obstructive pulmonary disease. *Am. J. Respir. Crit. Care Med.* **160**:S29–S32.
52. Pouladi, M.A., et al. 2004. Interleukin-13-dependent expression of matrix metalloproteinase-12 is required for the development of airway eosinophilia in mice. *Am. J. Respir. Cell Mol. Biol.* **30**:84–90.
53. Bonniaud, P., et al. 2004. Smad3 null mice develop airspace enlargement and are resistant to TGF-beta-mediated pulmonary fibrosis. *J. Immunol.* **173**:2099–2108.
54. Blackburn, M.R., Datta, S.K., and Kellems, R.E. 1998. Adenosine deaminase-deficient mice generated using a two-stage genetic engineering strategy exhibit a combined immunodeficiency. *J. Biol. Chem.* **273**:5093–5100.
55. Sun, D., et al. 2001. Mediation of tubuloglomerular feedback by adenosine: evidence from mice lacking adenosine 1 receptors. *Proc. Natl. Acad. Sci. U. S. A.* **98**:9983–9988.
56. Marquardt, D.L., Walker, L.L., and Heinemann, S. 1994. Cloning of two adenosine receptor subtypes from mouse bone marrow-derived mast cells. *J. Immunol.* **152**:4508–4515.
57. Knudsen, T.B., et al. 1992. Effects of (R)-deoxycoformycin (pentostatin) on intrauterine nucleoside catabolism and embryo viability in the pregnant mouse. *Teratology.* **45**:91–103.